



Cite this: *Phys. Chem. Chem. Phys.*,
2024, 26, 8761

Fragmentation of 5-fluorouridine induced by low energy (< 12 eV) electrons: insights into the radiosensitization of DNA

Paulina Wierzbicka,^a Hassan Abdoul-Carime^b and Janina Kopyra^{a*}

5-Fluorouracil is now routinely used in chemo- and radiotherapy. Incorporated within DNA, the molecule is bound to the sugar backbone, forming the 5-fluorouridine sub-unit investigated in the present work. For the clinical usage of the latter, no information exists on the mechanisms that control the radiosensitizing effect at the molecular level. As low energy (< 12 eV) electrons are abundantly produced along the radiation tracks during cancer treatment using beams of high energy particles, we study how these ballistic secondary electrons damage the sensitizing molecule. The salient result from our study shows that the *N*-glycosidic bonds are principally affected with a cross-section of approximately two orders of magnitude higher than the canonical thymidine, reflecting to some degree the surviving factor of radiation-treated carcinoma cells with and without 5-fluorouracil incorporation. This result may help in the comprehension of the radiosensitizing effect of the fluoro-substituted thymidine in DNA.

Received 29th September 2023,
Accepted 12th February 2024

DOI: 10.1039/d3cp04745h

rsc.li/pccp

Introduction

5-Fluorouridine (5FUrd) is a modified thymidine, in which the methyl (CH_3) group within the nucleobase sub-unit is surrogated by a fluorine atom (Fig. 1). In the past, halogenated nucleobases have been developed for their potential usage in cancer therapies. Indeed, in the late 1950s, it has been observed that bacterial cells containing DNA in which the canonical thymine was replaced by halogenated pyrimidine became more sensitive to ionizing radiation.¹ Among the studied halo-substituted nucleobases, only 5-fluorouracil (5FU) is yet commercially available² and routinely used clinically alone or in combination with other anticancer drugs in chemotherapy.³ When incorporated into DNA, 5FU is bound to the sugar backbone to form 5FUrd,⁴ enhancing damage in radiation therapy.⁵ It is also noteworthy that ^{18}F -5-fluorouridine is already known as a probe for measuring tissue proliferation and characterization of tumors in the PET (positron emission tomography) imaging technique.⁶

During radiation therapy, high energy particle beams produce along their tracks various secondary species (e.g., ions and radicals); among them, a large amount of ballistic electrons are produced.⁷ It is known from simulations and measurements that when considering only a single ionization event per

primary particle, the secondary electrons vs energy has a maximum around 9–10 eV.^{8,9} Subsequent secondary ionization processes can further shift the energy distribution to lower energies. It is now established that these slow particles are capable of damaging DNA in terms of single and double bond breakages¹⁰ and more locally they induce the rupture of the *N*-glycosidic bonds between the nucleobase and the (deoxy)ribose.¹¹ Moreover, substituting the canonical thymine by bromo-containing nucleobases within oligonucleotides sensitizes the modified-DNA strands to the ballistic electrons.¹² The fragmentation of halogenated nucleobases by low

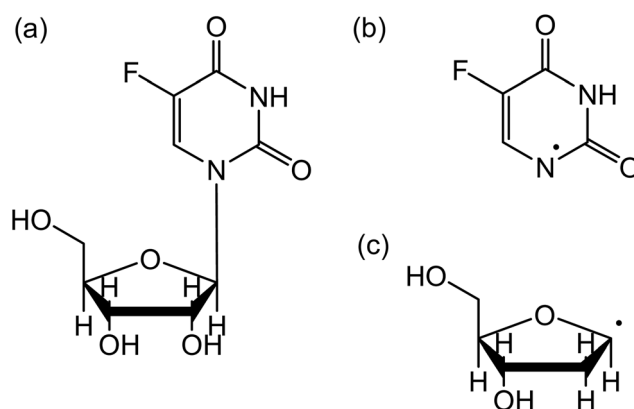


Fig. 1 Structure of 5-fluorouridine (5FUrd) (a). The molecule consists of (b) dehydrogenated 5-fluorouracil bound to (c) dehydrogenated ribose (or DNA sugar) via the *N*-glycosidic bond.

^a Faculty of Sciences, Siedlce University, 3 Maja 54, Siedlce 08-110, Poland.
E-mail: janina.kopyra@uws.edu.pl

^b Université de Lyon, Université Claude Bernard Lyon 1, CNRS, Institut Lumière Matière, UMR5306, Villeurbanne F-69622, France

energy electrons (LEEs) has been explored in the gas phase experiments.^{13–15} For 5-fluorouracil, it has been observed that electrons induce the fragmentation of the nucleobase into two predominant dissociation channels producing the dehydrogenated nucleobase anion and the OCN^- anion species, *via* resonant processes. The question is whether the fragmentation process reflects these observations when 5FU is bound to the deoxyribose moiety. Indeed, it has been reported that the fragmentation of thymine produces a large variety of anion fragments (*i.e.*, 9 fragment species),¹⁶ while once bound to the ribose moiety, the fragmentation of thymidine (Thd) by electrons in the same energy range generates only three fragments including the dehydrogenation of the nucleoside and the cleavage of the *N*-glycosidic bond with an excess electron residing in the thymine or sugar counterparts.^{17–19} Therefore, it is desirable to investigate the collision of 5FUrd for comparison with not only 5FU^{13–15} but also with Thd^{17–19} to deepen the understanding of the fragmentation mechanism and potentially the beneficial use of this molecule for the treatment of radiation therapy.

The present study aims to investigate the interaction of low energy (< 12 eV) electrons with 5-fluorouridine. We show the ability of such slow particles to fragment the molecule at energies as low as near 0 eV. Various fragmentation channels are observed; however, the three predominant pathways lead to the dehydrogenation of the halogenated nucleoside, the cleavage of the *N*-glycosidic bond, and the fragmentation of the sugar moiety. For the fragment anions generated through these pathways, we provide the values of the branching ratios and the cross-sections.

Experimental method

Electron collision experiments were performed using crossed electron-molecular beam apparatus.²⁰ The experimental setup consists of an electron source, an oven, and a quadrupole mass analyzer (Balzers QMA 140) that are housed in a UHV chamber at a base pressure of approximately 8×10^{-9} mbar. A quasi-monoenergetic electron beam generated from a trochoidal electron monochromator (a resolution of ≈ 250 meV FWHM and an electron current of approximately 10 to 20 nA), orthogonally intersected with an effusive molecular beam of 5-fluorouridine ($\geq 99\%$ purity powder, purchased from Sigma-Aldrich). The sample of 5-fluorouridine was used as received without further purification. The molecular beam was generated *via* the sublimation of the sample and heated by two *in vacuo* halogen bulbs. The temperature in the chamber was measured using a PT100 resistor, and the pressure of the investigated compound in the reaction area was around 7×10^{-7} mbar. The value of the decomposition temperature of 5-fluorouridine is 548 K.²¹ Since in our experiments the sample of 5-fluorouridine was heated at 433 K, that is to a temperature much lower than the decomposition temperature, it was assumed to have intact molecules in the gas phase for the present collision experiments.

Negative ions produced in the reaction area due to collision of electrons with intact molecules were extracted from the

interaction zone by a small draw-out-field ($< 1 \text{ V cm}^{-1}$) towards the QMA and detected using a single pulse counting technique. Prior to the measurements, the electron energy scale was calibrated by using the SF_6 gas flowing through the oven, yielding the well-known SF_6^- *s*-wave resonance near zero eV. However, the measurements were performed without the presence of the calibration gas, avoiding potentially unwanted reactions, such as dissociative electron transfer, with the investigated molecules producing an additional signal near 0 eV.²²

Results and discussion

Fig. 1 presents the structure of 5-fluorouridine studied in this work. It is composed of dehydrogenated fluorouracil (Fig. 1b, 5FU-H), bound to the *D*-ribofuranose (Fig. 1c, RNA sugar) moiety *via* a *N*-glycosidic bond. Fig. 2–5 exhibit anion yields of the fragment produced from electron impact as a function of the incident electron energy (*i.e.*, yield functions). As can be seen, three dissociation channels dominate molecular fragmentation, resulting in the formation of anion species at m/z 261, 129, and 45 (Fig. 2). From the stoichiometry, these anions can be assigned to the $(5\text{FUrd-H})^-$, $(5\text{FU-H})^-$ and HCOO^- fragment anions, respectively. The latter anion is likely to arise from the fragmentation of the *D*-ribofuranose moiety in analogy to the previous results from DEA to *D*-ribose.²³ Further fragment anions are also observed (Fig. 3–5), and all are listed in Table 1, with possible identification of their nature. It is likely that most of them are generated from the

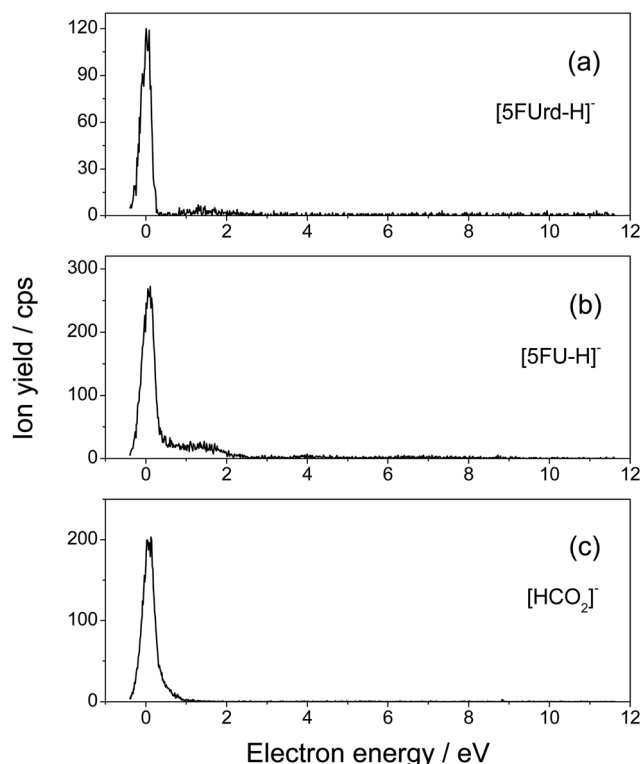


Fig. 2 Yield function of the (a) dehydrogenated parent anion $[5\text{FUrd-H}]^-$, (b) dehydrogenated 5-fluorouracil anion $[5\text{FU-H}]^-$ produced from the *N*-glycosidic bond cleavage, and (c) $[\text{HCO}_2]^-$ anion.

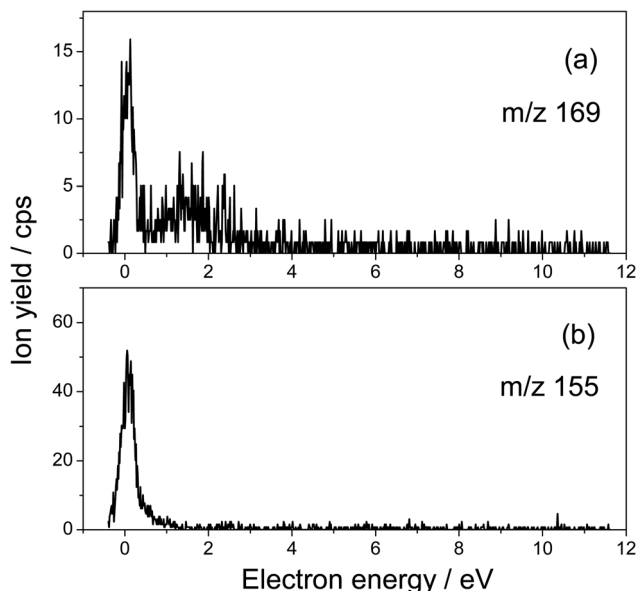


Fig. 3 Yield function of anions detected at (a) m/z 169 and (b) m/z 155.

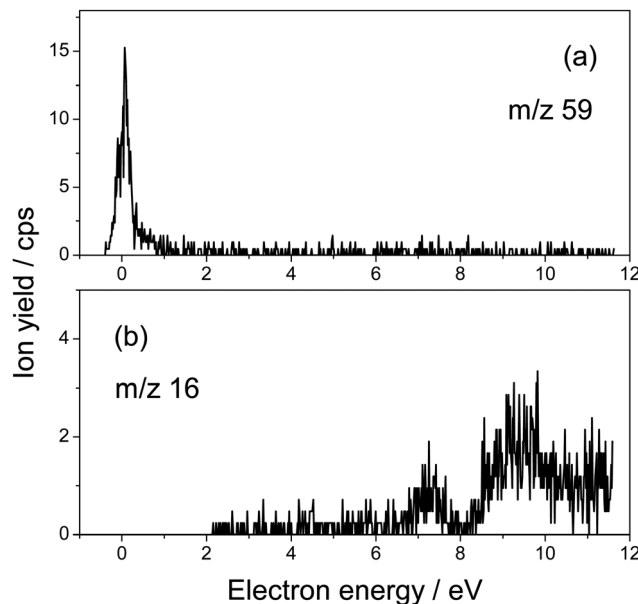


Fig. 5 Yield function of anions detected at (a) m/z 59 and (b) m/z 16.

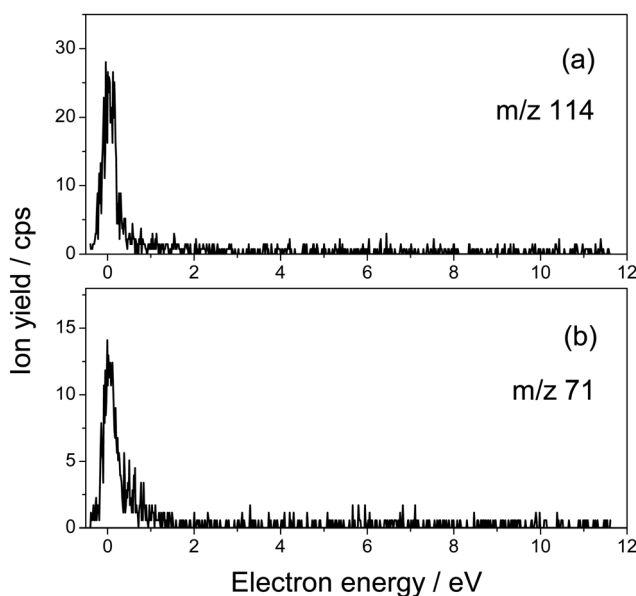


Fig. 4 Yield function of anions detected at (a) m/z 114 and (b) m/z 71.

fragmentation of the sugar moiety. The fragmentation of 5FUrd does not result in the formation of the same fragments as from DEA to 5FU.^{13–15} The observed fragmentation of 5FUrd differs from that reported earlier for thymidine, Thd.^{17,18} Indeed, previous works have shown that the dissociation of Thd by low-energy electrons produces dehydrogenated thymidine and thymine as well as sugar moiety anions, with the two latter species arising from the *N*-glycosidic bond cleavage.^{17,18,24} On the other hand, the present results show the production of (5FU-H)[−] and fluorine, F[−], anions (the signal of the latter is weak and not exploitable quantitatively). The present observations follow to some extent those from electron induced dissociation of 2′-

deoxy-5-bromouridine for which the dehydrogenated uracil anion ((5BrU-H)[−]) and Br[−] anion have been reported as the predominant fragments²⁵ or 2′-deoxy-5-fluorocytidine²⁶ for which the dehydrogenated cytosine anion ((5FC-H)[−]) as well as C₅H₆O₂[−] (m/z 98, generated due to the *N*-glycosidic bond cleavage and abstraction of a neutral water molecule with the charge remaining on the sugar unit) have been observed as the most prevalent fragment anions. It is also noted that similar to halogen-substituted nucleosides,^{23,26} the fragment anions are formed at very low electron energies (< 2 eV), particularly near 0 eV. The only exception is the formation of O[−] that was generated at a higher energy above 6 eV (see Fig. 5).

The anion yield functions shown in Fig. 2–5 exhibit structures indicating that the fragmentation of 5FUrd is controlled by a resonant process, *i.e.*, dissociative electron attachment (DEA).²⁷ Briefly, the incoming electron is captured in some virtual molecular orbitals (MOs) of the neutral molecule to form a transitory negative ion (TNI). This TNI undergoes dissociation into an anion fragment and a neutral counterpart if the dissociation time is shorter than the electron auto-detachment time (*i.e.*, survival probability). The peak position observed in the anion signal (Table 1) is obtained as a convolution of the electron capture in the resonance state cross-section and the survival probability.²⁵ Four states with a dissociative character (*i.e.*, σ^* or π^* decaying into σ^*) are reported: ~ 0.05 eV and ~ 1.4 eV for all negative fragments except for the O[−] anion, which exhibit peak positions at 7.4 eV and 9.5 eV. The very low-energy resonances, typically below ~ 4.5 eV (*i.e.*, first electronically excited state), usually arise from the shape resonance or the occupation of virtually unoccupied MOs by the excess electron.²⁸ At higher energies, the core-excited resonance prevails (*i.e.*, excitation of a valence electron to a MO concomitantly to the trapping of the excess electron by the positive core).²⁶ The production of all fragments is likely to arise from the shape resonance, except for

Table 1 The observed anion fragments, the tentative assessment of the species, and the peak positions, in eV. '⇒' suggest that fragmentation occurs at the ribose or at the nucleobase moiety. The values in parenthesis refer to the branching ratios at a given electron energy

<i>m/z</i>	Anion fragment assessment	Peak position
261	[5FUrd-H] [−]	0.01 (14.8)
169	[(5FU-H)C ₂ O] [−] (F-nucleobase + C ₂ O)	1.4 (2.3)
155	[(5FU-H)C ₂ H ₂] [−] (F-nucleobase + C ₂ H ₂)	0.07 (1.8)
129	[5FU-H] [−]	1.5 (57.0)
		0.07 (6.5)
114	[C ₅ H ₆ O ₃] [−] ⇒ sugar or [C ₄ H ₂ O ₄] [−] ⇒ sugar or [FC ₄ O ₂ NH] [−] ⇒ nucleobase	0.06 (37.4)
101	[C ₄ H ₅ O ₃] [−] ⇒ sugar	1.2 (40.7)
71	[C ₃ H ₃ O ₂] [−] ⇒ sugar or [C ₂ O ₂ NH] [−] ⇒ nucleobase	0.05 (3.4)
59	[C ₂ H ₃ O ₂] [−] ⇒ sugar	0.05 (5.8)
45	[HCO ₂] [−] ⇒ sugar	0.05 (1.7)
16	O [−]	0.06 (1.6)
		0.07 (27.0)
		7.4
		9.5

the O[−] anion, which is controlled by the core-excited resonance. The resonance at 7.4 eV has been calculated not only for glucose that partially implicates the σ* character of the C–O bonding of the molecule,²⁹ but also for the canonical nucleobase uracil.³⁰ The resonances below 2 eV, calculated for many nucleobases,^{31–33} have been suggested to arise from the excess electron captured into a π* orbital for forming the TNI. In particular, for thymidine, the TNI may further decay, *via* a fast transfer of the additional electron to the ribose (and ultimately to the phosphate) moiety for fragmentation, producing both the dehydrogenated nucleobase and the dehydrogenated ribose anion.^{14,15,34}

The three dominant anion fragments, that is (5FUrd-H)[−], (5FU-H)[−] and HCO₂[−], deserve particular discussion. For the dehydrogenated 5-flourouridine anion, the loss of a hydrogen atom may arise either from the nucleobase side through N–H or C–H bond cleavage or from the ribose side through C–H or O–H bond rupture. From the electron impact on thymidine,^{17,18} thymine^{14,35} and partially deuterated thymine,³⁶ it has been concluded that at electron energies below 2 eV, hydrogen is abstracted from the nitrogen site. Therefore, in the present experiment, the loss of hydrogen must also arise from the nitrogen site of the 5FUrd. The production of the (5FU-H)[−] anion arises from the rupture of the *N*-glycosidic bond, as has been reported for thymidine,^{17,18} 2'-deoxy-5-bromouridine,²³ and 2'-deoxy-5-fluorocytidine.²⁶ For thymidine, the cleavage of the N–H bond is energetically accessible due to the high electron affinity of the thymine moiety (~3.6–3.8 eV³⁷) with respect to the typical C–N bond dissociation energy (3.0–3.6 eV).³⁸ The HCO₂[−] anion can be assessed as a carboxylate and/or hydrocarboxyl anion, *i.e.* HCOO[−] or HOCO[−], respectively. Such an anion must arise from fragmentation of the ribose counterpart *via* at least a C–O and a C–C bond rupture. The HCOO radical, for which the electron affinity is higher, that is, 3.5 eV,³⁹ than that of the HOCO radical (1.51 eV (*cis*) and 1.37 eV (*trans*)),⁴⁰ is likely to drive the fragmentation process that must operate *via* complex atom rearrangements. Further fragments are also observed and we tentatively assess the nature of these anions (Table 1), suggesting that they arise mainly from the fragmentation of the sugar moiety. For these fragments listed in Table 1, we refrain from further speculation on the potential mechanisms by which they are produced.

Fig. 2–5 also show that, near 0 eV, molecular fragmentation leads to different competitive channels. By integrating the yield of each fragment near 0 eV, it is possible to estimate the branching ratios for each dissociative channel. The estimates are provided in Table 1 (in parentheses). For instance, three dominant (5FUrd-H)[−], (5FU-H)[−], and HCO₂[−] anionic fragments represent a total of 79.2% of the all fragmentation channels at this energy (*i.e.*, 14.8%, 37.4% and 27%, respectively). Molecular dissociation can be quantified by the evaluation of the DEA cross-section for each fragmentation channel. In the first approximation, the number of measured ions by our experiment, irrespective to their nature, *N*_{ions}, can be estimated as: *N*_{ions} = ε·*N*_e·(*N*_{mol}/*V*)σ·*L*, where ε is the detection efficiency (assuming the same for all ions), *N*_e represents the number of electrons (or current), *N*_{mol}/*V* is the density of the target molecule (proportional to the injected gas pressure), σ is the ion production cross-section and *L* is the collision length. Thus, the relative fragmentation cross-section can also be estimated by comparing the integrated yield of the negative ion with that of the calibration gas, SF₆[−], σ_{ion}/σ_{SF6}. We have evaluated the relative cross-sections for the production of the (5FUrd-H)[−], (5FU-H)[−], and HCO₂[−] fragment anions to be 0.0027, 0.075 and 0.055, respectively, within 30% accuracy from the reproducibility of our measurements. Knowing the cross-section for the formation of the SF₆[−] anion at 420 K (*c.a.*, ~9 × 10^{−14} cm²),^{41,42} the DEA cross-sections for the production of these anions can be derived to be 2.4 × 10^{−15} cm², 6.8 × 10^{−15} cm² and 5.0 × 10^{−15} cm², respectively. For comparison, the cross-section for the *N*-glycosidic bond dissociation of thymidine producing the dehydrogenated thymine anion has been estimated to be 4 × 10^{−17} cm² (430 K).¹⁴ Here, the cross-section for the (5FU-H)[−] anion production estimated at 433 K (*c.a.*, 1.1 × 10^{−15} cm² within 50% accuracy) is about 170 times higher than that for thymidine. It should be noted that since the local temperature in the vicinity of the ionizing track may locally increase dramatically above 400 K,⁴³ the present measurements may be relevant to the evaluation of the local damage of the nucleoside. Finally, the fragmentation cross-section is temperature dependent and may possibly drop by two orders of magnitude at biologically relevant temperatures.⁴⁴

Conclusions

The present results demonstrate the capacity of low energy (< 12 eV) electrons to decompose 5-fluorouridine producing various fragments, for which the three most dominant channels operate through (1) the loss of a hydrogen radical, (2) the cleavage of the *N*-glycosidic bond producing a highly reactive abasic sugar radical, and (3) the fragmentation of the sugar moiety. Furthermore, the analysis of the results in Table 1 suggest that, in terms of the number of fragments, the dissociation of 5FUrd arises to a large extent from the ribose moiety, while the fluoro-nucleobase appears to be less fragmented. It should also be noted that with the exception of O^- all the generated fragment anions are formed at very low electron energies (< 2 eV). These results differ from the electron-5FU collision experiments for which fragmentation leads to various species of significant intensity, e.g., OCN^- and CN^- at electron energies above 2 eV,¹⁴ indicating the fragility of the fluoro-substituted nucleobase towards LEEs.

The generated mobile hydrogen radical concomitantly to the formation of the $(5FUrd-H)^-$ anion may further react with the neighboring molecules, while the damage at the sugar moiety may result in a scission of the DNA strand.⁴⁵ It is established that the formation of the reactive sugar radical favors the DNA strand break.^{46,47}

The present work also shows that the cross-section for the cleavage of the *N*-glycosidic bond in 5FUrd, induced by LEEs, is found to be approximately two orders of magnitude higher than that in thymidine, providing valuable information for radiosensitization observation of a halogen surrogate of the canonical thymine. Indeed, this value of ratio is high, but not surprising, and it reflects to some degree the surviving fraction measured for radiation treated carcinoma cells with and without 5FU substitution,⁴⁸ assuming the different experimental conditions and the systems studied, that is, the cell vs. model subunit of DNA. For example, it has been shown that ^{60}Co radiation treatment of HT29 carcinoma cells containing 5-fluorouracil with a dose of above 5 Gy led to a drop in the cell survival factor by two orders of magnitude or more.⁴⁸ Finally, in a more realistic environment, i.e., in the presence of surrounding water, it is likely that the main dissociation channels, which include the glycosidic bond cleavage reported from the present gas phase experiments, also arise, as it has been reported that the quasi-free electrons induce *N*-glycosidic bond dissociation of ribothymidine in the 18–22 MeV pulse radiolysis experiment,¹¹ and the local temperature in the vicinity of the ionizing track may increase above 400 K.⁴³

Conflicts of interest

There are no conflicts to declare.

Acknowledgements

J. K. acknowledges support by a statutory activity subsidy (No 141/23/B) from the Polish Ministry of Science and Higher Education. This study was supported by Agence Nationale de

la Recherche (ANR) (grant number 18-CE30-0009-03). The research was conducted in the frame of the COST action CA18212 Molecular Dynamics in the GAS phase (MD-GAS) and action CA20129 “MultiChem”.

References

- 1 S. Zamenhof, R. de Giovanni and S. Greer, *Nature*, 1958, **181**, 827.
- 2 e.g., Fluorouracil Pfizer®, <https://www.pfizer.fr/medicaments-home/fluorouracile-pfizer>.
- 3 J. Gu, Z. Li, J. Zhou, Z. Sun and C. Bai, *Oncol. Lett.*, 2019, **18**, 2091–2101.
- 4 C. McMahon, F. Catez, N. Della Venezia, F. Vanhalle, L. Guyot, A. Vincent, M. Garcia, B. Roy, J.-J. Diaz and J. Guitton, *J. Pharm. Anal.*, 2021, **11**, 77–87.
- 5 J. H. Lu, T.-H. Tsai, Y. J. Chen, L. Y. Wang, H. Y. Liu and C. H. Hsieh, *Front. Pharmacol.*, 2020, **11**, 141.
- 6 E. J. Crawford, M. Friedkin, A. P. Wolf, J. S. Fowler, B. M. Gallagher, R. M. Lambrecht, R. R. McGregor, C. Y. Shiue, I. Wodinski and A. Goldin, *Adv. Enzyme Regul.*, 1982, **20**, 3–22.
- 7 i.e., 1.5×10^4 electrons per deposited 500 keV. ICRU report 31, Average energy required to produce an ion pair, International Commission of Radiation Units and Measurements, Bethesda (1979).
- 8 F. Blanco, A. Munõz, D. Almeida, F. Ferreira da Silva, P. Limaõ-Vieira, M. C. Fuss, A. G. Sanz and G. Garcia, *Eur. Phys. J. D*, 2013, **67**, 199.
- 9 M. Mücke, M. Braune, M. Förstel, T. Lischke, V. Ulrich, T. Arion, U. Becker, A. Bradshaw and U. Hagenhahn, *Nat. Phys.*, 2010, **6**, 143–146.
- 10 B. Boudaiffa, P. Cloutier, D. Hunting, M. A. Huels and L. Sanche, *Science*, 2000, **287**, 1658–1660.
- 11 J. Ma, A. Kumar, Y. Mutoya, S. Yamashita, T. Sakurai, S. A. Denisov, M. D. Sevilla, A. Adhikari, S. Seki and M. Mostafavi, *Nat. Commun.*, 2019, **10**, 102.
- 12 H. Abdoul-Carime, P. C. Dugal and L. Sanche, *Radiat. Res.*, 2000, **153**, 23–28.
- 13 H. Abdoul-Carime, M. A. Huels, E. Illenberger and L. Sanche, *J. Am. Chem. Soc.*, 2001, **123**, 5354–5355.
- 14 H. Abdoul-Carime, M. A. Huels, E. Illenberger and L. Sanche, *Int. J. Mass Spectrom.*, 2003, **228**, 703–716.
- 15 E. Arthur-Baidoo, G. Schöpfer, M. Oncak, L. Chomicz-Manka, J. Rak and S. Denifl, *Int. J. Mol. Sci.*, 2022, **23**, 8325.
- 16 S. Denifl, S. Ptasinska, M. Probst, J. Hrusak, P. Scheier and T. D. Märk, *J. Phys. Chem. A*, 2004, **108**, 6562–6569.
- 17 H. Abdoul-Carime, S. Gohlke, E. Fischbach, J. Scheike and E. Illenberger, *Chem. Phys. Lett.*, 2004, **387**, 267–270.
- 18 S. Ptasinska, S. Denifl, S. Gohlke, P. Scheier, E. Illenberger and T. D. Märk, *Angew. Chem., Int. Ed.*, 2006, **45**, 1893–1896.
- 19 Y. Zheng, P. Cloutier, D. J. Hunting, R. Wagner and L. Sanche, *J. Am. Chem. Soc.*, 2004, **126**, 1002–1003.
- 20 J. Kopyra, *Phys. Chem. Chem. Phys.*, 2012, **14**, 8287–8289.
- 21 P. Singh, G. Tyagi, R. Mehrotra and A. K. Bakhshi, *Drug Test. Anal.*, 2009, **1**(5), 240–244.

- 22 S. Gohlke, H. Abdoul-Carime and E. Illenberger, *Chem. Phys. Lett.*, 2003, **380**, 595–599.
- 23 I. Bald, J. Kopyra and E. Illenberger, *Angew. Chem., Int. Ed.*, 2006, **45**, 4851.
- 24 S. A. Krasnokutski, A. Y. Ivanov, V. Izvekov, G. G. Sheina and Y. P. Blagoi, *J. Mol. Struct.*, 1999, **482–483**, 249–252.
- 25 H. Abdoul-Carime, P. Limão-Vieira, I. Petrushko, N. J. Mason, S. Gohlke and E. Illenberger, *Chem. Phys. Lett.*, 2004, **393**, 442–447.
- 26 J. Kopyra, A. Keller and I. Bald, *RSC Adv.*, 2014, **4**, 6825–6829.
- 27 T. F. O'Malley, *Phys. Rev.*, 1966, **150**, 14–29.
- 28 E. Illenberger and J. Momigny, *Gaseous Molecular Ions. An Introduction to Elementary Processes Induced by Ionization*, Steinkopff Verlag, Darmstadt/Springer-Verlag, New York, 1992.
- 29 R. F. da Costa, M. H. F. Bettega, M. T. do N. Varella and M. A. P. Lima, *J. Chem. Phys.*, 2010, **132**, 124309.
- 30 A. Dora, J. Tennyson, L. Bryjko and T. van Mourik, *J. Chem. Phys.*, 2009, **130**, 164307.
- 31 X. Li, L. Sanche and M. D. Sevilla, *J. Phys. Chem. B*, 2004, **108**, 5472–5476.
- 32 P. V. Shchukin, M. V. Muftakhov, R. V. Khatymov and R. F. Tuktarov, *J. Chem. Phys.*, 2022, **156**, 104304.
- 33 F. Kossocki, M. H. F. Bettega and M. T. D. N. Varella, *J. Chem. Phys.*, 2014, **140**, 024317.
- 34 J. Berdys, P. Skurski and J. Simons, *J. Phys. Chem. B*, 2004, **108**, 5800–5805.
- 35 H. Abdoul-Carime, S. Gohlke and E. Illenberger, *Phys. Rev. Lett.*, 2004, **92**, 1681063.
- 36 S. Ptasinska, S. Denifle, B. Mroz, M. Probst, V. Grill, E. Illenberger, P. Scheier and T. D. Märk, *J. Chem. Phys.*, 2005, **123**, 124302.
- 37 S. Denifle, S. Ptasinska, G. Hanel, G. G. G. Stir, M. Probst, P. Scheier and T. D. Märk, *J. Chem. Phys.*, 2004, **120**, 6557–6565.
- 38 T. H. Lowry and K. S. Richardson, *Mechanism and Theory in Organic Chemistry*, Harper Collins Publications, New York, 3rd edn, 1987.
- 39 E. Garand, K. Klein, J. F. Stanton, J. Zhou, T. I. Yacovitch and D. M. Neumark, *J. Phys. Chem. A*, 2010, **114**, 1374–1383.
- 40 C. J. Johnson, M. E. Harding, B. L. J. Poad, J. F. Stanton and R. E. Continetti, *J. Am. Chem. Soc.*, 2011, **133**, 19606–19609.
- 41 L. G. Christophorou and J. K. Olthoff, *J. Phys. Chem. Ref. Data*, 2000, **29**, 267–330.
- 42 L. G. Christophorou and J. K. Olthoff, *Adv. Atom. Mol. Opt. Phys.*, 2001, **44**, 155–293.
- 43 E. Surdurevich, E. Scifoni and A. V. Solov'yov, *Mut. Res.*, 2010, **704**, 206–212.
- 44 J. Kopyra and H. Abdoul-Carime, *J. Chem. Phys.*, 2015, **142**, 174303.
- 45 W. Knapp Pogożelski and T. D. Tullius, *Chem. Rev.*, 1998, **98**, 1089–1108.
- 46 C. von Sonntag, *The chemical basis of radiation biology*, Taylor & Francis, London, 1987.
- 47 M. Dizdaroglu, C. von Sonntag and D. Schulte-Frohlinde, *J. Am. Chem. Soc.*, 1975, **97**, 2277–2278.
- 48 T. S. Lawrence, M. A. Davis and J. Maybaum, *Int. J. Radiat. Oncol., Biol., Phys.*, 1994, **29**, 519–523.